INTERNATIONAL JOURNAL FOR NUMERICAL METHODS IN FLUIDS, VOL. 22, 211–221 (1996)

COMPUTATION OF DILUTE PARTICULATE LAMINAR FLOW OVER A BACKWARD-FACING STEP

I. E. BARTON

Division of Aerospace Engineering, Manchester School of Engineering, Manchester University, Oxford Road, Manchester M13 9PL, U.K.

SUMMARY

Particle-laden flows are calculated for a classical laminar backward-facing step problem. The particle tracks are calculated using a recently developed exponential Lagrangian tracking scheme. The behaviour of the particle-laden flow is considered for various inlet for Reynolds number, Stokes numbers and void fractions. Doping the flow with low-Stokes-number particles has the effect of increasing the inlet inertia of the flow and this increases the strength of the recirculation behind the step. High-Stokes-number particles are dominated by gravitational effects which affect the flow accordingly. Differences between the single-phase flow and the particle-laden flows are therefore dependent on the Stokes number and increase linearly with void fraction.

KEY WORDS: backward-facing step; particle-laden flow; Lagrangian tracking

INTRODUCTION

Flow separation is a fundamental phenomenon in fluid mechanics. Particle-laden flows are also an interesting phenomenon ranging from engineering processes to arterial systems. The present study investigates these phenomena by numerically predicting the behaviour of laminar particle-laden flow over a backward-facing step. Laminar flow over a backward-facing step is probably one of the simplest forms of flow separation. The backward-facing step geometry used in the present study has become a classical numerical benchmark, initiated by the numerical study of Armaly *et al.*[1] which included an experimental investigation. The geometry of the backward-facing step has an upper solid boundary above the step which simplifies the numerical boundary conditions. The laminar predictions by Armaly *et al.*[1] were fairly poor compared with the experimental data owing to an inadequate grid density, whilst subsequent hydrodynamic numerical predictions found good agreement with the experimental data provided that the three-dimensional experimental effects are not significant.[2–5] The effects of the step height have been studied by Thangam and Knight[6,7] and the viscous drag from the upper boundary by Barton.[8] The problem has also been used to address numerical issues such as grid adaptation[9,10] and boundary conditions.[11,12] Laminar particle-laden flows have not been studied for the present geometry (to the best of the author's knowledge), although turbulent particle-laden flows for the geometry have been experimentally studied by Ruck and Makiola.[13] The effect of the particles on the flow is assumed to be negligible because of the low number density of the particles.

The present study considers how the particles introduced into the flow affects its behaviour. Different types of particles, aerodynamically classified by their Stokes number, affect the flow differently and the Stokes number is varied accordingly. The perturbation of the flow by the particles

CCC 0271–2091/96/030211–11

Received January 1995
Revised May 1995

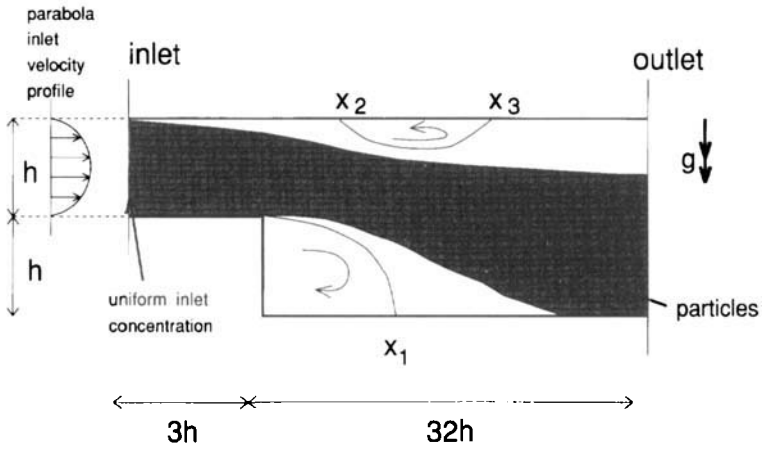

Figure 1. Geometry of backward-facing step problem illustrating recirculation regions and presence of particles

increases with the number density, which is also demonstrated in the present study. The problem and geometry are summarized in Figure 1. The channel expands forming the backward-facing geometry with an expansion ratio of 1:2. An entrance channel of $3h$ is used to prevent downstream effects travelling upstream, where h is the height of the step. The main channel is $32h$ long. The figure also illustrates the reattachment and separation lengths x_1, x_2 and x_3.

In the following sections the basic equations and solution procedure for the particulate two-phase flow are presented. The fluid phase is solved using the SIMPLE method[14] which is discussed initially. The particle phase is solved using Lagrangian tracking and the effects of the particles on the flow field are introduced via source terms.

GOVERNING EQUATIONS

The governing equations for the fluid phase are the equation of continuity and the Navier–Stokes equations in two dimensions with some additional source terms:

$$\frac{\partial u}{\partial x}+\frac{\partial v}{\partial y}=0, \tag{1}$$

$$\frac{\partial \rho u^2}{\partial x}+\frac{\partial \rho uv}{\partial y}=\frac{\partial p}{\partial x}+\mu\left(\frac{\partial^2 u}{\partial x_2}+\frac{\partial^2 u}{\partial y^2}\right)+S_{\mathrm{p}}^{u}, \tag{2}$$

$$\frac{\partial \rho uv}{\partial x}+\frac{\partial \rho v^2}{\partial y}=-\frac{\partial p}{\partial y}+\mu\left(\frac{\partial^2 v}{\partial x_2}+\frac{\partial^2 v}{\partial y_2}\right)+S_{\mathrm{p}}^{v}. \tag{3}$$

The only source terms necessary are the terms S_{p}^{u} and S_{p}^{v} which describe the interaction between the fluid and solid phases. In the Lagrangian approach for particle-laden flows the volume of the particles is neglected and only if the particle volume changes will there be a source term for the equation of continuity. The principle of using source terms to describe the interaction between phases was proposed by Migdal and Agosta[15] and developed into the particle-source-in-cell (PSIC) method.[16] Alternatively, a particulate continuum model using the Eulerian approach could be used, but this method has the disadvantage that particles experience a dispersion effect caused by numerical diffusion.[17] As Brownian motion and diffusion effects have been ignored in the present study, the PSIC

method was considered more suitable. The PSIC method has become a well-established method for calculating particle-laden flows particularly for engineering problems.[18]

The numerical solution of the fluid phase is based on a solution procedure developed for single-phase flows developed by Patankar and Spalding.[19] The partial differential equations (1–3) are integrated over control volumes which form a computational grid over the problem domain. The grid used in the present study is shown in Figure 2. The grid uses 100 × 80 grid points. The size of the control volumes varies over the problem domain, with clustering of control volumes close to solid boundaries. The grid dependence was tested by comparing the reattachment and separation positions with coarser grids. The present reattachment and separations results are estimated to have an accuracy of about 1% (the greatest error is associated with the separation position x_2). The velocity and pressure terms are located on a staggered grid system developed for the marker-and-cell (MAC) method.[20] The solution procedure requires interpolation between various points, which is achieved by a quadratic upwind differencing scheme.[21] The discretized equations are solved in an iterative procedure starting with the solution of the velocities using the current pressure field. Thereafter the pressure correction equation is solved which is derived from the equation of continuity. The pressure correction terms relate to velocity correction terms, which means that the pressure and velocity fields can be corrected so that they satisfy continuity. The whole procedure is repeated until the velocity and pressure fields converge to a final solution. The convergence criterion requires the velocity and pressure residuals to reduce by five orders of magnitude. The results were solved on a Hewlett-Packard workstation 9000/700. The CPU time for a fully converged solution ranged from 3 to 9 h, increasing with Reynolds number for the single-phase solutions. The two-phase solutions were not solved directly, instead, the single-phase solutions were initially used and the inlet void fraction was gradually increased. The CPU time required to integrate and store a single-particle trajectory was about 0·7 s. The discretized equations were solved using a tridiagonal matrix solution algorithm[22] sweeping from the inlet to the outlet boundary.

The inlet velocity terms are prescribed using a u-velocity parabolic profile. The outlet velocity terms are found by first-order extrapolation, which is relatively inaccurate but stable;[23] however, the inaccuracy is reduced by placing the outlet condition some way downstream of the regions of interest. No-slip boundary conditions are applied at the solid boundaries.

The particulate phase is solved using the equation of motion for a single particle. The equation of motion for the particles can be described using the Basset–Boussinesq–Oseen equation.[24] The present

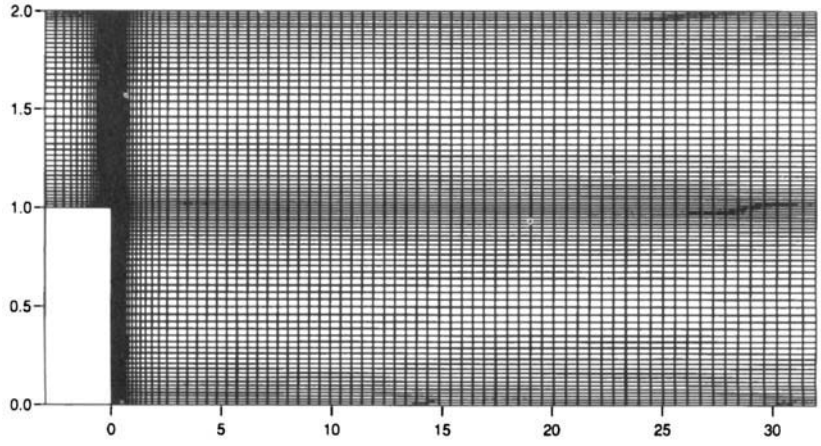

Figure 2. Computational grid

study assumes that the particle is heavier than the surrounding fluid and that the equation of motion can be reduced to a modified Stokes law and the gravitational force[25]

$$m_p \frac{du_p}{dt} = 3\pi\mu d_p f(u_f - u_p) + m_p\left(1 - \frac{\rho_f}{\rho_p}\right)g, \tag{4}$$

where m_p is the mass of the particle and d_p is the diameter of the particle. The coefficient f describes the influence of the ultra-Stokesian drag:[25]

$$f = 1 + 0{\cdot}15Re_p^{0{\cdot}687}. \tag{5}$$

The term Re_p is the particle Reynolds number:

$$Re_p = \frac{\rho d_p |u_f - u_p|}{\mu}. \tag{6}$$

The equation of motion can then be integrated to find the velocity of the particle and the particle position. The particle initially starts at a location on the inlet boundary. The equation of motion is integrated using a recently developed predictor–corrector exponential Lagrangian tracking scheme which is summarized in the Appendix. The global truncation error of the predictor–corrector exponential Lagrangian scheme is $O(\Delta t^2)$, whereas the standard exponential Lagrangian scheme has a global error of $O(\Delta t)$.

The particle momentum source terms S_p^u and S_p^v are derived from the transfer of momentum between phases due to the drag force. This means that a control volume has an extra source term described by the time integral across the control volume:

$$S_p^{u,v} = -3\pi\mu d_p \dot{n}_s \int_{t_{in}}^{t_{out}} f(u_f - u_p)\, dt, \tag{7}$$

where the times t_{in} and t_{out} are when the particle enters and leaves the control volume respectively. The term $\dot{n}_s$ is the number of particles travelling along a particle track per second. This can be expressed as

$$\dot{n}_s = \frac{6\alpha^{INLET} u_p^{INLET} \Delta y}{\pi d_p^3 N_L}. \tag{8}$$

The term u_p^{INLET} is the particle inlet velocity, which is set to be the same as the surrounding fluid velocity. The term Δy is the height of the inlet control volume and N_L is the number of starting positions in the control volume. The term α^{INLET} is the inlet void fraction, which is set to be uniform across the inlet. The void fraction is defined as

$$\alpha = \frac{V_p}{V}, \tag{9}$$

where V_p is the volume the particles displace in a unit of volume V.

The particle-laden flow is calculated by modifying the single-phase solution procedure previously discussed. This is achieved by incorporating the calculations of the particle velocity and trajectories into the source terms that form a particle source field, which acts on the flow field in a similar manner as the pressure field. The source term field needs to be continuous in the flow domain to achieve convergence. The source terms were dampened using underrelaxation to prevent divergence. This is a similar approach to that used by Durst *et al.*[26]

In order to achieve a continuous source field, a fairly large number of particle tracks have to be used. Most of the calculations in the present study used 10–20 particle starting locations per grid node.

The present study considered various inlet Reynolds numbers, Stokes numbers and void fractions. The ratio of the particle density to the fluid density is 10, which is sufficient to allow the present assumption that drag and gravity are the only significant forces. The inlet Reynolds number was varied from $Re = 50$ to 700, similar to other numerical studies. The Stokes numbers studied varied from 1×10^{-5} to 1×10^{-1}. The Stokes number is defined as

$$Stk = \frac{\rho_p d_p^2 u_o}{18\mu(2h)}, \tag{10}$$

where u_0 is the average inlet velocity and $2h$ is the main channel height. The Stokes number was sufficiently low to prevent high particle Reynolds numbers which would invalidate the steady state laminar behaviour of the flow. The present study was concerned with studying the effects of changing the flow from the single-phase flow with increasing void fractions; the inlet void fraction was varied from 1×10^{-6} to 5×10^{-3}; also, the single-phase flow was predicted.

RESULTS

Single-phase flow

As discussed in the Introduction, the laminar single-phase flow problem has been extensively studied. The behaviour of the flow is briefly summarized below; for further details about the flow see References 1, 6 and 7; see Reference 5 for a presentation of pressure fields. The flow behaves similarly to an open backward-facing step flow for low Reynolds numbers: the flow separates at the step and reattaches downstream at position x_1. The position x_1 increases almost linearly; the slight non-linear trend is caused by viscous drag along the upper boundary.[8] For higher Reynolds numbers the adverse pressure gradient is strong enough to create an upper recirculation region which is illustrated in Figure 1. The upper recirculation region increases in size with increasing Reynolds number and its core moves downstream. The reattachment and separation positions are summarized in Figure 3 together with the experimental data of Armaly *et al.*;[1] the results of Guj and Stella[4] are also shown for a numerical comparison. For low Reynolds numbers the present predictions are in good agreement with the experimental data, but for higher Reynolds numbers the numerical predictions start to deviate from the

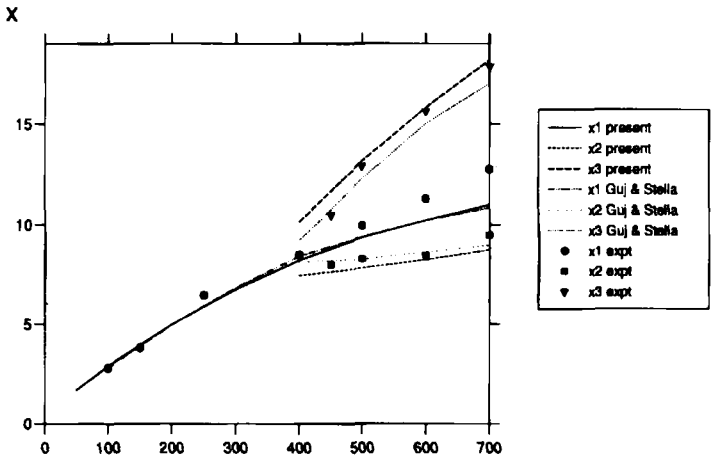

Figure 3. Variation in reattachment and separation lengths with inlet Reynolds number for single-phase flow

experimental data. The differences are probably caused by three-dimensional effects present in the experiment.

Particle-laden flows

The presence of the particles in the flow has, in the present study, the main parameters of Stokes number and inlet void fraction. The behaviour of the various results is considered by setting one of these parameters to a constant value and varying the other.

The particles are introduced to the flow at the inlet; this has a significant effect on the low-Stokes-number particle results. Since low-Stokes-number particles are not affected by gravitational forces, then if a particle is initially assumed to be in a recirculation region, it will remain there and the void fraction will become uniform throughout the domain. However, if a low-Stokes-number particle is assumed to enter the flow at the inlet, it will not enter the recirculation regions provided that there is no exchange force such as Brownian motion. The current study takes the very idealistic view that no dispersion forces are present and therefore no particles should be present in the recirculation regions for very low Stokes numbers.

Variation in Stokes number. The behaviour of the flow is dependent on the Stokes number: low-Stokes-number particles tend to follow the flow, which has the effect of reinforcing the freestream of the flow. This is because the inertia of the low-Stokes-number particles tend to be too small to allow the particles to penetrate the recirculation regions. The particles passing over the lower recirculation region have the effect of driving the lower recirculation region, which increases its size and vorticity. As the particles are not greatly affected by gravity, the increased lower recirculation region tends to reduce the adverse pressure gradient along the upper boundary. High-Stokes-number particles have a higher inertia and their behaviour is mostly affected by their initial velocity and the gravitational force. The gravitational force acts downwards as shown in Figure 1, similar to the study by Ruck and Makiola.[13] As the high-Stokes-number particles are dominated by the effects of gravity, the behaviour of the flow is dependent on its direction of acceleration. The gravity force tends to make the particles deposit along the lower boundary and also within the lower recirculation region. This has a compression effect on the lower recirculation region and reduces its size. The downward movement of the particles encourages flow downwards along the channel. The downward movement increases the size of the upper recirculation region. The separation length x_2 moves upstream with increasing Stokes number owing to the smaller lower recirculation region and the induced downward flow.

The behaviour of the low- and high-Stokes-number particles is examined for $Re = 400$ and $\alpha^{\mathrm{INLET}} = 5 \times 10^{-4}$ in Figure 4. The figure shows the variation in the reattachment and separation lengths with Stokes number. The reattachment and separation lengths for the single-phase flow are also shown in Figure 4 (broken lines) for a comparison with the particle-laden flow. The particle-laden flow has either larger or smaller lengths x_1 and x_2 depending on the Stokes number. The values tend to intersect at a Stokes number between 1×10^{-3} to 1×10^{-2}, which will be referred to as the *critical* Stokes number. The particle-laden flow length x_3 is nearly always bigger than the single-phase flow length. This is because the upper recirculation region is either forced downstream by the low-Stokes-number particles or increased in size by the high-Stokes-number particles.

At a higher Reynolds number a similar variation is observed and the variation in the reattachment and separation lengths with Stokes number is shown in Figure 5 for $Re = 600$ and $\alpha^{\mathrm{INLET}} = 3 \times 10^{-3}$. Again the critical Stokes number is between 1×10^{-3} to 1×10^{-2}. In this case the particle-laden flow length x_3 is always bigger than the single-phase flow length and remains fairly constant.

Deposition rates along the lower boundary after the sudden expansion remain constant along the channel. The deposition rate along the lower boundary is directly proportional to the Stokes number

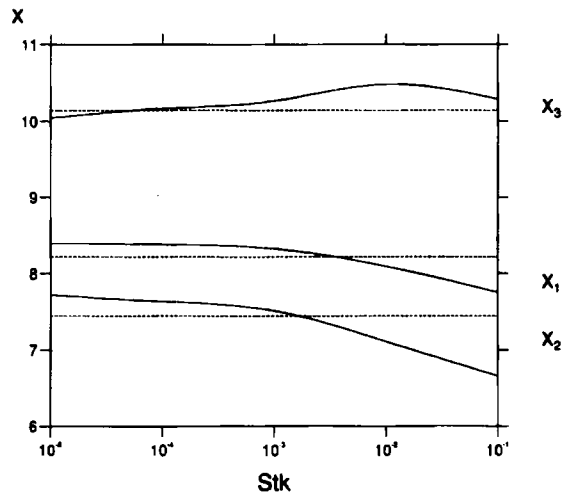

Figure 4. Variation in reattachment and separation lengths with Stokes number for $Re = 400$ and $\alpha^{INLET} = 5 \times 10^{-4}$

(except for very large Stokes numbers where a considerable number of particles deposit in the inlet channel). Large-Stokes-number particle deposition rates decrease slightly near the sudden expansion, because the settling velocity is significant in comparison with the flow reversal in the recirculation region.

Variation in void fraction. The most important parameter in terms of the behaviour of the particles is the Stokes number; the differences caused by varying the void fraction are, however, dependent on the Stokes number. Varying the void fraction simply has the effect of increasing the differences which are dependent on the Stokes number. Obviously, low-void-fraction results tend to single-phase results and void fractions of 1×10^{-6} were found to give the same solution as the single-phase results. As the critical Stokes number is between $Stk = 1 \times 10^{-3}$ and 1×10^{-2}, the variation in the reattachment and separation lengths is examined for $Stk = 1 \times 10^{-3}$ and 1×10^{-2} in Figures 6 and 7 respectively for $Re = 400$. The figures show how the differences increases with void fraction, where the

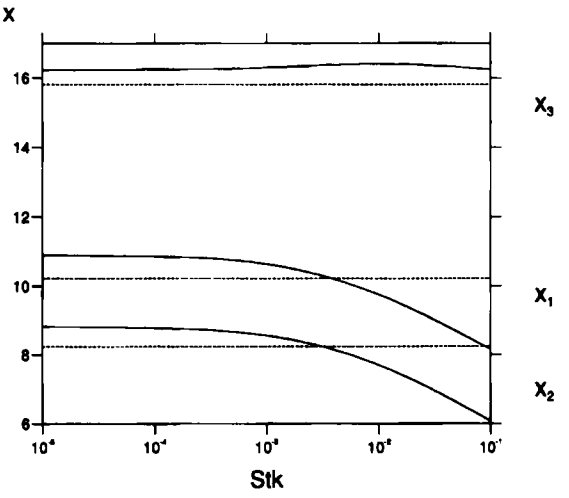

Figure 5. Variation in reattachment and separation lengths with Stokes number for $Re = 600$ and $\alpha^{INLET} = 3 \times 10^{-3}$

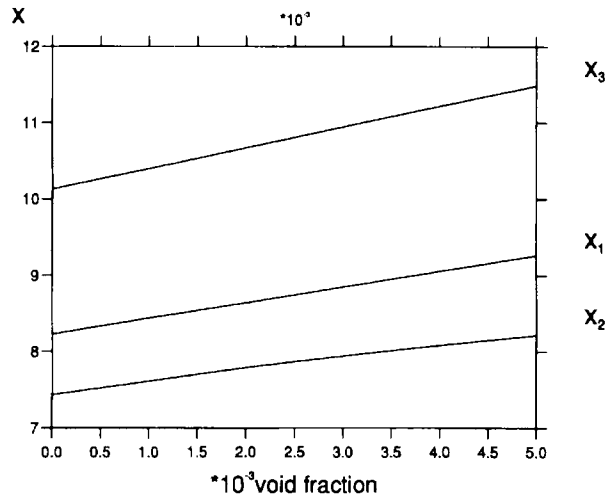

Figure 6. Variation in reattachment and separation lengths with void fraction for $Re = 400$ and $Stk = 1 \times 10^{-3}$

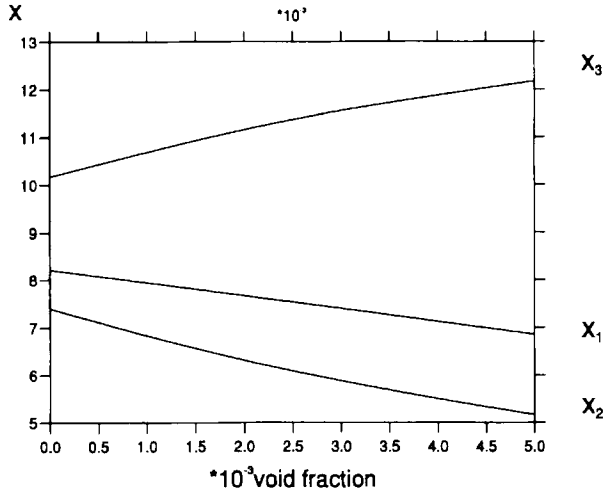

Figure 7. Variation in reattachment and separation lengths with void fraction for $Re = 400$ and $Stk = 1 \times 10^{-2}$

$Stk = 1 \times 10^{-3}$ particles drive the lower recirculation region and the $Stk = 1 \times 10^{-2}$ particles shorten the lower recirculation region and increase the size of the upper recirculation region.

The behaviour of the particles is reflected in the concentration plots of void fractions in Figures 8 and 9 for $\alpha = 3 \times 10^{-3}$, $Re = 400$ and $Stk = 1 \times 10^{-3}$ and 1×10^{-2} respectively (black for $\alpha = 3 \times 10^{-3}$). The figures clearly show how the 1×10^{-2} Stokes number particles penetrate the lower recirculation region. The particles that penetrate are then pulled upstream by the recirculation region. The penetration of the lower recirculation region is caused by the gravitational force and by the upper recirculation region forcing particles downwards. Elsewhere in the channel the gravitational force has only a slight effect, which can be observed in Figure 9 in the region $x = 16$–20 where the downward movement is small. The 1×10^{-3} Stokes number particles tend to stay in the main body of the flow. The particles are forced slightly downwards by the upper recirculation region and they fail to recover completely. A small number of particles enter the lower recirculation region near the lower

Figure 8. Concentration field of void fraction for $Re = 400$, $Stk = 1 \times 10^{-3}$ and $\alpha^{INLET} = 3 \times 10^{-3}$

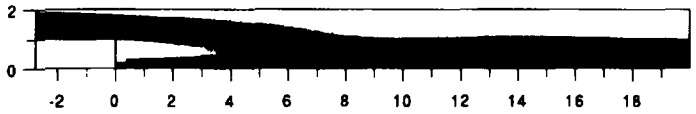

Figure 9. Concentration field of void fraction for $Re = 400$, $Stk = 1 \times 10^{-2}$ and $\alpha^{INLET} = 3 \times 10^{-3}$

reattachment; they are transported upstream in the recirculation region almost all the way up to the backward-facing step wall.

Inlet Reynolds number. Different inlet Reynolds number results show that the particles have a fairly uniform effect on the flow except for very low Reynolds numbers. The $Re = 400$ results vary five times more than the $Re = 100$ results in terms of changes in reattachment and separation lengths. This is because the flow has such a small recirculation region and there is consequently only a small effect that can be caused by the behaviour of the particles. However, the behaviour of the particles varies greatly for low Reynolds numbers from particles depositing in the entrance channel to particles being carried successfully in the core of the flow and passing over the lower recirculation region.

The medium Reynolds-number flows in the range $Re = 400$–500 are probably the most affected by the introduction of particles, partly because the mean stream velocity is strong enough to successfully transport low-Stokes-number particles and yet it fails to do so for higher-Stokes-number particles and also because the lower recirculation region is sufficiently large to be appreciably affected by the variation in the particle behaviour. In comparison, higher-Reynolds-number flows tend to successfully transport the particles past the lower recirculation region and the differences caused in the separation and reattachment lengths remains fairly constant. Higher-Reynolds-number flows therefore tend to produce constant deposition rates along the lower boundary, decreasing in magnitude with Reynolds number. The deposition rate near the sudden expansion is slightly lower for low-Reynolds-number flows for the same reason that high-Stokes-number particle profiles tend to decrease.

CONCLUDING REMARKS

Laminar particle-laden flows were calculated for a classical backward-facing step geometry. The Stokes number and void fraction were varied and several inlet Reynolds numbers were considered.

The Stokes number of particles has a fundamental effect on the flow. Low-Stokes-number particles are successfully transported in the main body of the flow and this reinforces the inertia of the flow. In the present study this has the effect of increasing the lower recirculation region and decreasing the upper recirculation region. High-Stokes-number particles are dominated by their initial inlet velocity and the gravitational force. In the present study the particles tend to deposit on the lower boundary, compressing the lower recirculation region. The induced downward flow and smaller lower recirculation region increase the size of the upper recirculation region.

Increasing the void fraction simply increased the expected differences from the single-phase flow. The differences are dependent on the Stokes number.

Low-Reynolds-number flows vary greatly in behaviour with changes in Stokes number, but because of their small recirculation regions, changes in the lower reattachment length are usually quite small

compared with moderate-Reynolds-number flows. Higher-Reynolds-number flows tend to successfully transport the particles even with high Stokes numbers through the main channel.

APPENDIX

The equation of motion for a particle can be assumed to be of the form

$$\frac{\partial u_p}{\partial t} = \frac{u_f - u_p}{\tau_p} + g, \tag{11}$$

where u_p is the particle velocity, u_f is the displaced fluid velocity, g is the gravitational term (which could be zero) and τ_p is the particle relaxation time (which may be modified owing to ultra-Stokesian drag). The integration of the equation is achieved by assuming that u_f varies quadratically over the present and previous time step. It can therefore be expressed in the form

$$u_f(t) = u_f^n + At + Bt^2,$$

$$A = \frac{u_f^{n+1^*}(\Delta t^{n-1})^2 + u_f^n((\Delta t^n)^2 - (\Delta t^{n-1})^2) - u_f^{n-1}(\Delta t^n)^2}{\Delta t^{n-1}\Delta t^n(\Delta t^{n-1} + \Delta t^n)}, \tag{12}$$

$$B = \frac{u_f^{n-1}\Delta t^n + u_f^{n+1^*}\Delta t^{n-1} - u_f^n(\Delta t^n + \Delta t^{n-1})}{\Delta t^{n-1}\Delta t^n(\Delta t^{n-1} + \Delta t^n)},$$

where the superscript n refers to the current time level. The term $u_f^{n+1^*}$ is the predicted fluid velocity at the next time level. The scheme initially predicts the particle position by assuming a constant fluid velocity over the time step, e.g. $A = 0$ and $B = 0$. The term $u_f^{n+1^*}$ can then be predicted and the scheme next predicts the particle position assuming the above quadratic temporal variation. The particle position is re-predicted and the term $u_f^{n+1^*}$ is updated. The procedure is repeated once more and the particle velocity and position are calculated.

The general solutions of the particle velocity and position are expressed as

$$U_p^{n+1} = U_p^n \exp\left(\frac{-\Delta t}{\tau_p}\right) + U_f^n\left[1 - \exp\left(\frac{-\Delta t}{\tau_p}\right)\right] + A\left\{\Delta t - \tau_p\left[1 - \exp\left(\frac{-\Delta t}{\tau_p}\right)\right]\right\}$$

$$+B\left\{\Delta t^2 - 2\tau_p\Delta t + 2\tau_p^2\left[1 - \exp\left(\frac{-\Delta t}{\tau_p}\right)\right]\right\} + \tau_p\left[1 - \exp\left(\frac{\Delta t}{\tau_p}\right)\right]g, \tag{13}$$

$$x_p^{n+1} = x_p^n - \tau_p(U_f^n - U_p^n)\left[1 - \exp\left(\frac{-\Delta t}{\tau_p}\right)\right] + U_f^n\Delta t + A\left\{\frac{\Delta t^2}{2} - \tau_p\Delta t + \tau_p^2\left[1 - \exp\left(\frac{-\Delta t}{\tau_p}\right)\right]\right\}$$

$$+B\left\{\frac{\Delta t^3}{3} - \tau_p\Delta t^2 + 2\tau_p^2\Delta t - 2\tau_p^3\left[1 - \exp\left(\frac{-\Delta t}{\tau_p}\right)\right]\right\} + \tau_p\left\{\Delta t + \tau_p\left[1 - \exp\left(\frac{-\Delta t}{\tau_p}\right)\right]\right\}g. \tag{14}$$

REFERENCES

1. B. F. Armaly, F. Durst, J. C. F. Pereira and B. Schönung, 'Experimental and theoretical investigation of backward-facing step flow', *J. Fluid. Mech.*, **127**, 473–496 (1983).
2. J. Kim and P. Moin, 'Application of a fractional-step method to incompressible Navier–Stokes equations', *J. Comput. Phys.*, **59**, 308–323 (1985).

3. P. Orlandi, 'Vorticity–velocity formulation for high *Re* flows', *Comput. Fluids*, **15**, 137–149 (1987).
4. G. Guj and F. Stella, 'Numerical solutions of high-*Re* recirculating flows in vorticity–velocity form', *Int. j. numer. methods fluids*, **8**, 405–416 (1988).
5. J. L. Sohn, 'Evaluation of FIDAP on some classical laminar and turbulent benchmarks', *Int. j. numer. meethods fluids*, **8**, 1469–1490 (1988).
6. S. Thangam and D. D. Knight, 'Effect of stepheight on the separated flow past a backward facing step', *Phys. Fluids*, **1**, 604–606 (1989).
7. S. Thangam and D. D. Knight, 'A computational scheme in generalized coordinates for viscous incompressible flows', *Comput. Fluids*, **18**, 317–327 (1990).
8. I. E. Barton, 'Laminar flow past an enclosed and open backward-facing step', *Phys. Fluids*, **6**, 4054–4056 (1994).
9. J. F. Hétu and D. H. Pelletier, 'Adaptive remeshing for viscous incompressible flows', *AIAA J.*, **30**, 1986–1992 (1992).
10. D. Lee and Y. M. Tsuei, 'A hybrid adaptive gridding procedure for recirculating fluid flow problems', *J. Comput. Phys.*, **108**, 122–141 (1993).
11. D. K. Gartling, 'A test problem for outflow boundary conditions—flow over a backward-facing step', *Int. j. numer. methods fluids*, **11**, 953–967 (1990).
12. R. L. Sani and P. M. Gresho, 'Résumé and remarks on the open boundary condition minisymposium', *Int. j. numer. methods fluids*, **18**, 983–1008 (1994).
13. B. Ruck and B. Makiola, 'Particle dispersion in a single-sided backward-facing step flow', *Int. J. Multiphase Flow*, **14**, 787–800 (1988).
14. S. V. Patankar, *Numerical Heat Transfer and Fluid Flow*, Hemisphere, Washington, DC, 1980.
15. D. Migdal and V. D. Agosta, 'A source flow model for continuous gas–particle flow', *Trans. ASME, J. Appl. Mech.*, **34**, 860–865 (1967).
16. C. T. Crowe, M. P. Sharma and D. E. Stock, 'The particle-source-in-cell (PSI-cell) model for gas–droplet flows', *Trans. ASME, J. Fluids Eng.*, **99**, 325–332 (1977).
17. C. T. Crowe, 'Review—numerical models for dilute gas–particle flows', *Trans. ASME, J. Fluids Eng.*, **104**, 297–303 (1982).
18. F. C. Lockwood, A. P. Salooja and S. A. Syed, 'A prediction method for coal-fired furnaces', *Combust. Flame*, **38**, 1–15 (1980).
19. S. V. Patankar and D. B. Spalding, 'A calculation procedure for heat, mass and momentum transfer in three-dimensional parabolic flows', *Int. J. Heat Mass Transfer*, **15**, 1787–1806 (1972).
20. F. H. Harlow and J. E. Welch, 'Numerical calculation of time-dependent viscous incompressible flow', *Phys. Fluids*, **8**, 2182–2189 (1965).
21. B. P. Leonard, 'A stable and accurate convective modelling procedure based on quadratic upstream interpolation', *Comput. Methods Appl. Mech. Eng.*, **19**, 59–98 (1979).
22. D. A. Anderson, J. C. Tannehill and R. H. Pletcher, *Computational Fluid Mechanics and Heat Transfer*, Heimsphere, Washington, DC, 1984.
23. M. Peric, 'A finite volume method for the prediciton of three-dimensional fluid flow in complex ducts', *Ph.D. Thesis*, Mechanical Engineering Department, Imperial College, London, 1985.
24. M. R. Maxey and J. J. Riley, 'Equation of motion for a small rigid sphere in a nonuniform flow', *Phys. Fluids A*, **26**, 883–889 (1983).
25. R. Clift, J. R. Grace and M. E. Weber, *Bubbles, Drops and Particles*, Academic, New York, 1978.
26. F. Durst, D. Milojevic and B. Schönung, 'Eulerian and Lagrangian predictions of particle two-phase flows: a numerical study', *Appl. Math. Model.*, **8**, 101–115 (1984).